Efficient luminescence from AlP/GaP neighboring confinement structure with AlGaP barrier layers

F. Issiki
Research Center for Advanced Science and Technology (RCAST), The University of Tokyo, 4-6-1 Komaba, Meguro-ku, Tokyo 153, Japan

S. Fukatsu
Department of Pure and Applied Sciences, The University of Tokyo, 3-8-1 Komaba, Meguro-ku, Tokyo 153, Japan

Y. Shiraki
Research Center for Advanced Science and Technology (RCAST), The University of Tokyo, 4-6-1 Komaba, Meguro-ku, Tokyo 153, Japan

(Received 16 March 1995; accepted for publication 12 June 1995)

Highly efficient photoluminescence (PL) was observed from a new class of AlP/GaP quantum-confined geometry, neighboring confinement structure (NCS). The PL intensity of AlP/GaP NCSs was even higher than that of a 300-period AlP/GaP superlattice (SL), and the PL of the NCS exhibited much improved immunity against thermal quenching compared to SLs. The luminescence origin of the NCS was confirmed from the well width dependence of the PL peak shift. The peak shifts were compared with the calculation within the effective mass approximation using the previously reported band parameters for AlP and GaP. © *1995 American Institute of Physics.*

Luminescence efficiency is a central issue when we discuss optical properties of semiconductors. Extensive studies have recently been reported on *indirect gap* $Al_xGa_{1-x}P$ systems. In particular, much effort has been devoted to AlP/GaP superlattices (SLs)[1–5] chiefly motivated by the prediction of highly efficient luminescence through the zone-folding effect.[6–8] In contrast, little has been studied on luminescence from simplified structures as represented by the quantum well (QW).[9] Such a simple geometry offers an advantage in the context of materials growth in that a better crystalline quality is plausibly obtained when compared with much more complicated structures such as SLs, even with the existence of lattice mismatch. Another advantage is that the nonradiative recombination induced by carrier scattering at the heterointerfaces would be greatly reduced. As a matter of fact, strained $Si_{1-x}Ge_x$ QWs have exhibited PL efficiency no smaller than that of SLs with an extended period of more than 100.[10,11] Hence, there still seems to remain a possibility that the luminescence intensity of an $Al_xGa_{1-x}P$ heterostructure QW would greatly exceed those of SLs.

In this study, we present a comparative luminescence study for type-II $Al_xGa_{1-x}P$ QW systems and SLs, and the observation of an unexpectedly high efficiency of luminescence for $Al_xGa_{1-x}P$ QWs with type-II band lineup. It is shown that the PL intensity of $Al_xGa_{1-x}P$ QWs is higher than that of a 300-period SL.

The band lineup of the $Al_xGa_{1-x}P$/GaP system has been shown to be of type II (staggered), and the bottom of the conduction band is located at the X point, i.e., the Brillouin zone boundary in the k space, over the entire composition range.[12] Therefore, the radiative recombination is essentially of indirect nature both in real space and k space. The staggered band lineup has been regarded as the drawback of the $Al_xGa_{1-x}P$/GaP system since the oscillator strength of the optical transition is significantly reduced due to spatial separation of electrons and holes unlike the type-I systems.

To overcome such a limitation, we propose a new class of quantum confinement structure hereafter referred to as the *neighboring confinement structure* (NCS), where electrons and holes are separately confined in thin neighboring layers. The schematic band lineup of an AlP/GaP NCS is illustrated in Fig. 1. The confining layers (thin AlP and GaP layers) are cladded between $Al_xGa_{1-x}P$($x \approx 0.5$) barrier layers. The electrons are confined in the AlP layer, while the holes are confined in the GaP layer. The outer $Al_xGa_{1-x}P$ layers are essential to establish carrier buildup at the centered heterointerface. Then, the wave function penetration of the electrons and holes into the neighboring layers sets in as the thickness of the confining layers (AlP and GaP) is decreased. The increased overlap of the wave functions is expected to lead to an increased recombination probability of the electrons and holes and hence enhanced luminescence. Moreover, the excitonic binding would further strengthen the recombination probability due to enhanced overlap of the wave functions through Coulomb attraction.

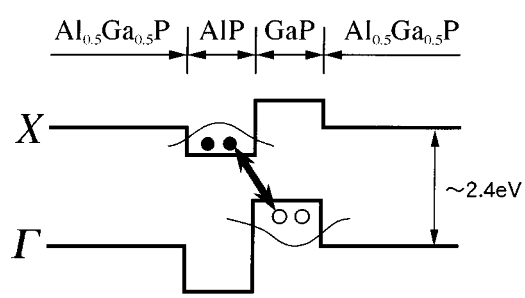

FIG. 1. Schematic band lineup of the AlP/GaP neighboring confinement structure (NCS). Note the increased envelope wave function penetration of the electrons and holes confined in NCS across the centered interface. The insertion of the symmetry-breaking AlP layer induces the conduction band Γ-X mixing, which facilitates the no-phonon recombination.

 0003-6951/95/67(8)/1048/3/$6.00

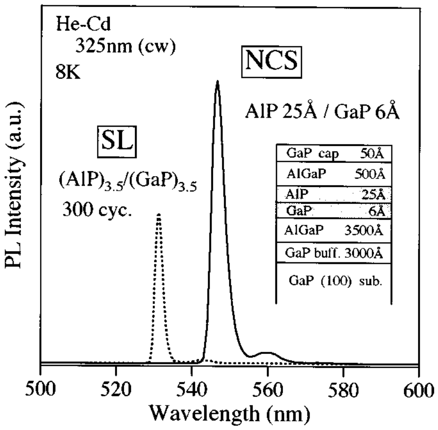

FIG. 2. 6 K PL spectra of the AlP 25 Å/GaP 6 Å NCS (solid line) and the control AlP/GaP SL (dashed line). The PL intensity of the NCS is higher, which shows an enhanced efficiency of the NCS luminescence. The inset shows the schematic sample structure of the NCS.

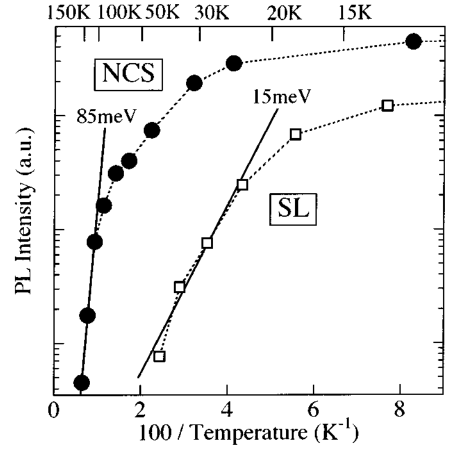

FIG. 3. Temperature dependence of the PL intensity of the NCS and the SL. Intensity of the NCS sample decreases only $\sim 10^{-1}$ times even at 100 K, while that of the SL sample is completely quenched at 50 K. The activation energies of the thermal rolloff for the NCS and the SL are 85 and about 15 meV, respectively.

A calculation within the effective mass approximation shows that, for an AlP 15 Å/GaP 15 Å NCS sandwiched between the $Al_xGa_{1-x}P$ of $x=0.5$, the normalized overlap integral of the envelope wave functions becomes more than 30%, which is fairly close to that of a type-I QW. This is of sufficient magnitude to compensate for the loss of the otherwise smaller transition probability inherent to the AlP/GaP type-II system due to real-space wave function separation.

In addition, we expect significant Γ-*X* mixing of the wave functions due to breakdown of the translational symmetry, which is induced by the introduction of thin AlP and GaP layers. This effectively relaxes the strict selection rule of the momentum-conserving optical transitions and allows for the dominance of no-phonon transitions. The present scheme can also be applied to material systems consisting of the type-II band lineup such as strained $Si_{1-x}Ge_x$ lattice matched to SiGe.[13–15]

All the samples were grown by gas source molecular beam epitaxy (GSMBE) (VG Semicon V80H) using PH_3 and elemental Ga and Al. The substrates are nominally undoped GaP(100) wafers. The sample structure of AlP 25 Å/GaP 6 Å NCS is shown in the inset of Fig. 2. After the growth of a 3500 Å buffer layer, the barrier layers and active layers were grown at around 620 °C, which is the minimum temperature that 4× patterns in the reflection high energy electron diffraction (RHEED) can be observed during the growth of the GaP buffer layer. This helps prevent thickness fluctuation of the GaP layer. During the growth of the GaP cap layer, the substrate temperature was ramp raised to 650 °C and the whole structure was annealed for 5 min. The composition of the $Al_xGa_{1-x}P$ barrier was confirmed to be within the range of $0.50<x<0.56$ from x-ray diffraction spectra. The control SL was a 300-period AlP/GaP SL separately grown at a substrate temperature of 700 °C, and its structure was confirmed to be $(AlP)_{3.5}/(GaP)_{3.5}$ from the satellite peak analysis of x-ray diffraction.

Figure 2 compares the PL spectra of the NCS (solid line) and the 300-period AlP/GaP SL (dashed line). The exciton source is a cw He–Cd laser (325 nm). The laser power density is 1.0 W/cm^2 and its total power is 20 mW. It is clearly seen that the PL intensity of the NCS is higher than that of the SL control, though the NCS is essentially a *single* heterostructure. There are no other pronounced features other than the dominant, main *no-phonon* line centered at 5465 Å in the PL spectrum of the NCS sample, except for a small phonon replica on the lower energy side.

Figure 3 shows the temperature dependence of the PL intensity of the NCS (circles) and the SL (squares). The exciting laser is focused to give a power density of 25 W/cm^2, causing the appearance of a shoulder on the higher energy side. The PL intensity is spectrally integrated, including the shoulder. This shoulder is thought to be due to free excitons, since the relative intensity of the shoulder increases with increasing temperature and it dominates at higher temperatures. Therefore the PL in Fig. 2 may be of a bound and/or localized exciton nature. The PL intensity of the NCS decreases only by a factor of 10 as the temperature is increased up to 100 K, whereas that of the SL is completely quenched at 50 K. The activation energy of the PL intensity rolloff at higher temperatures for the NCS is 85 meV, which is much improved over that for the SL, approximately 15 meV. Thus, the NCS is seen to offer better immunity against thermal quenching than the SL.

To confirm that the luminescence origin of the NCS is due to the expected spatial indirect transition, we grew two series of multiple NCS (MNCS) samples. In the first set of the samples, the GaP layer thickness was varied from 7 to 22 Å, while the AlP layer thickness was fixed at 20 Å. In the second set, the AlP layer thickness was varied as 13–50 Å, while keeping the GaP layer thickness at 10 Å. It is expected that the MNCS shows a quantum-confined peak shift as the thickness of AlP and GaP is varied.

The 6 K PL spectra from the two MNCS samples are shown in Fig. 4. The peaks clearly shift towards a higher energy side with decreasing thickness of the AlP and GaP layers. The maximum confinement shifts of 155 and 100 meV are obtained in the valence band (GaP) and conduction band (AlP), respectively. This is clear evidence that lumines-

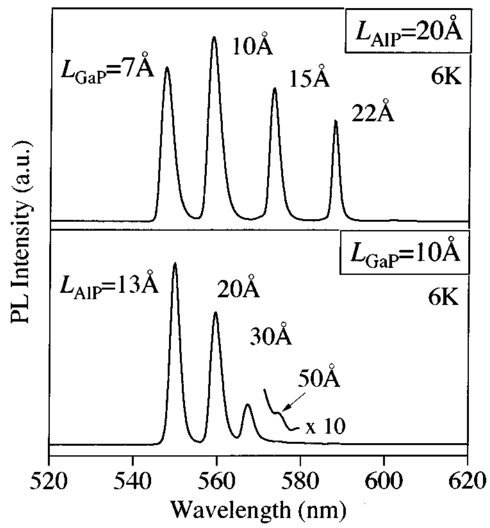

FIG. 4. 6 K PL spectra of the MNCSs. The peaks shift with changing AlP and GaP layer thickness, which reflects the quantum confinement in the conduction and valence bands, respectively.

cence of the NCS originates from the optical transition as sketched in Fig. 1.

Finally, we compared these experimental peak shifts with a calculation within the effective mass approximation on the basis of a single band envelope function approach. Figure 5 shows the well width dependence of the experimental peak energies (triangle and square dots) and the calculated peak energy (solid and dashed lines). In the calculation, the band parameters of AlP and GaP quoted in the previous literature ($E_{g_{\mathrm{GaP}}}=2.35$ eV (optical band gap),[16] $E_{g_{\mathrm{AlP}}}=2.51$ eV (optical band gap),[17] $\Delta E_v=0.43$ eV (RT),[18] $m_{\mathrm{GaP}_e^*}=0.25m_0$,[19] $m_{\mathrm{GaP}_h^*}=0.45m_0$,[20] and $m_{\mathrm{AlP}_h^*}=0.51m_0$[21] (where m_0 is the free electron mass) were used. The effective masses and the band gap are cited from Ref. 22. $\Delta E_c=0.27$ eV is calculated as $\Delta E_c=\Delta E_v+E_{g_{\mathrm{GaP}}}-E_{g_{\mathrm{AlP}}}$ Linear interpolation was used to obtain the compositional dependence of the $\mathrm{Al}_x\mathrm{Ga}_{1-x}\mathrm{P}$ parameters. Exceptionally, since the electron effective mass $m_{\mathrm{AlP}_e^*}$ of AlP is not well established, it is treated instead as a fitting parameter in the calculation. The tendency of the experimental peak shift agrees well with the calculation, though the energy offset of 105 meV is necessary for the perfect agreement of the absolute peak position with the experiment. The best fit is obtained with $m_{\mathrm{AlP}_e^*}\approx 0.4m_0$, which seems to be a reasonable value. The large energy offset of 105 meV still needs justification and warrants re-examination of the validity of the effective mass approximation.

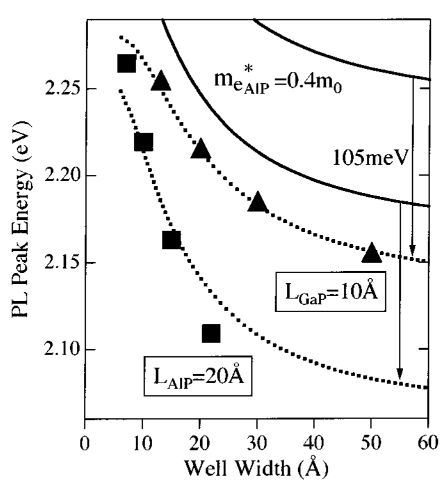

FIG. 5. The experimented and calculated well width dependencies of the PL peak energy. The square and triangle dots are the experimental peak energies shown in Fig. 4. The dashed lines are the calculated peak shift on the supposition of $m_{\mathrm{AlP}_e^*}\approx 0.4m_0$, offset by 105 meV downward from the solid lines that are calculated using the reported band gap.

The observed PL intensity of the NCS was one order of magnitude lower than that of the GaAs/AlGaAs QW, but the green luminescence was still clearly visible to naked eye.

In conclusion, we propose a new class of AlP/GaP quantum-confined geometry, NCS, and observed efficient luminescence with considerable immunity against thermal quenching compared to SLs. The well width dependence of the PL of the NCS was investigated, and the luminescence origin of the NCS was confirmed.

The authors gratefully acknowledge the support and instructions of crystal growth provided by Y. Seko, and the technical support of S. Otake and T. Ohta. This work was supported in part by a Grant-in-Aid from Ministry of Science, Education and Culture, Japan. One of the authors (S. F.) gratefully acknowledges Torray Science Foundation, Asahi Glass Foundation, and the Murata Science Foundation, Japan.

[1] A. Morii, H. Okagawa, K. Hara, J. Yoshino, and H. Kukimoto, J. Cryst. Growth **124**, 772 (1992).
[2] A. Morii, I. Ohno, A. Kanda, K. Arai, K. Tokudome, K. Hara, J. Yoshino, and H. Kukimoto, Jpn. J. Appl. Phys. **30**, L1244 (1991).
[3] K. Asami, H. Asahi, T. Watanabe, S. Gonda, H. Okumura, and S. Yoshida, Surf. Sci. **267**, 450 (1990).
[4] A. Sasaki, Xue-Lun Wang, and A. Wakahara, Appl. Phys. Lett. **64**, 2016 (1994).
[5] X. L. Wang, A. Wakahara, and A. Sasaki, Appl. Phys. Lett. **62**, 888 (1993).
[6] Y. Tanida and M. Ikeda, Phys. Rev. B **B50**, 10958 (1994).
[7] M. Kumagai, T. Takagahara, and E. Hanamura, Phys. Rev. B **B37**, 898 (1988).
[8] G. Shibata, T. Nakayama, and H. Kimura, Jpn. J. Appl. Phys. **33**, 6121 (1994).
[9] T. Takano, H. Fukushima, S. Koshihara, F. Minami, T. Nagao, T. Fujimori, and H. Goto (unpublished).
[10] U. Menczigar, G. Abstreiter, J. Olajos, H. Grimmeiss, H. Kibbel, H. Presting, and E. Kasper, Phys. Rev. B **B47**, 4099 (1993).
[11] S. Fukatsu, Solid-State Electron. **37**, 817 (1994) and references therein.
[12] Zh. I. Alferov, D. Z. Garbuzov, S. G. Konnikov, P. S. Kop'ev, and V. A. Mishurnyi, Sov. Phys. Semicond. **7**, 1449 (1974).
[13] R. People, IEEE J. Quantum Electron. **22**, 1696 (1986).
[14] G. Abstreiter, H. Brugger, T. Wolf, H. Jorke, and H. J. Herzog, Phys. Rev. Lett. **54**, 2441 (1985).
[15] N. Usami, F. Issiki, D. K. Nayak, Y. Shiraki, and S. Fukatsu (unpublished).
[16] R. G. Humphreys, U. Rössler, and M. Cardona, Phys. Rev. B **18**, 5590 (1978).
[17] B. Monemar, Phys. Rev. B **8**, 5711 (1973).
[18] J. R. Waldrop, R. W. Grant, and E. A. Kraut, J. Vac. Sci. Technol. B **11**, 1617 (1993).
[19] N. Miura, G. Kido, M. Suekane, and S. Chikazumi, J. Phys. Soc. Jpn. **52**, 2838 (1983).
[20] J. R. Chelikowsky and M. L. Cohen, Phys. Rev. B **14**, 556 (1976).
[21] Landolt-Börnstein, *Numerical Data and Functional Relationships in Science and Technology*, edited by O. Madelung (Springer, Berlin, 1987), Group III, Vol. 22.